

# Influence of Tip Roughness and Application Area on Tip Vortex Pressure

Christian Krüger, Nikolai Kornev, Mathias Paschen, Christian Semlow

University of Rostock, Chair of Modelling and Simulation  
Albert-Einstein-Str. 2  
D-18055 Rostock

christian.krueger@uni-rostock.de

## Introduction

Modern shipbuilding and development shows a strong demand for highly efficient and powerful propulsion systems. Moreover, tendencies of maximizing the cargo hold leads to decreasing space provided for the propulsion system. On the downside of this progression are highly tip-loaded propellers. This can lead to prominent tip vortex structures and subsequently forwarding to frequent tip vortex cavitation, hull excitation and rudder erosion.

Within a joint research project of MMG Waren GmbH and the University of Rostock an innovative approach has been investigated claiming the possibility of perturbing propeller tip vortices by a roughened propeller tip region.

## Theoretical Background

In marine propulsion tip vortices come to mind especially when showing up in its extreme occurrence, forming a cavitating vortex helix. Even though erosion, induced by tip vortex cavitation, in general does not impact on the propeller itself, the harmful effects on installations placed downstream like rudders are quite remarkable [3]. Furthermore, the comfort conditions are affected as well. Hull excitation and underwater noise [9], arising from increased 2<sup>nd</sup> order pressure fluctuations, are challenges of modern propeller design.

The approach, for delaying or modifying tip vortex structures and cavitation for wing configurations by technical solutions is fairly old. Besides the familiar aspects of classic propeller design, one may know for instance the propeller tip vane by Vatanabe [7], ducted tips or bulbous tips [6], to name but a few. With each solution having its individual benefits, it is obvious that application for retrofit becomes difficult, if cavitation characteristics and customers expectations does not comply.

In lights of this, the investigations of Katz and Galdo [4] pointed out a distinct relation between surface roughness and tip vortex roll-up for a rectangular hydrofoil, demonstrating a shift in detachment point and a substantial reduction in tip vortex strength due to increasing surface roughness. Based on these results, Johnsson and Ruttgeron [1] studied the influence of leading edge roughness on the tip vortex roll-up for different angles of attack. It was shown, that application of roughness on the pressure side near the leading edge has a delaying effect on tip vortex cavitation. On the downside of these results was an increase in drag up to 10% due to the highly exposed roughened area causing a total decrease in efficiency by 2%.

Philipp and Ninnemann [5] suggested, that small scale turbulence perturbation within the boundary layer, caused by surface roughness, may result in a destabilizing of the tip vortex structure. They claimed the back on the suction side of the propeller tip to be the most efficient application area. Cavitation tunnel experiments proved a scattered cavitating vortex structure and a decrease of 2<sup>nd</sup> order pressure fluctuations of 35% accompanied by a lowering of open water efficiency of 2.5%.

An evidence for the connection between turbulence of the outer flowfield and vortex core dynamics was given by the work of Hussain and Pradeep [2], pointing out that the eigenmodes of the evolving vortex allow resonance effects with the relatively weak outer turbulence leading to perturbation amplification by several orders of magnitude.

## Numerical Setup

A blade model based on the P1380 cavitation tunnel experiments of the Potsdam Model Basin was designed, providing an equal thrust distribution within translational flow as its rotational counterpart. Using the chord-, skew- and thickness distribution of the original P1380, the blade sections were straightening into horizontal plane. Using symmetric sections, the original camber distribution was reset. The pitch distribution was found impressing the calculated thrust distribution  $F_{A,des}$  of the original P1380 propeller to the translational model using a panel code for solving the equations

$$\Delta F_{A,j} = \left[ F_{A,des,j} - \sum_{i=1}^N \left( \frac{\partial F_{A,j}}{\partial \alpha_i} \alpha_i \right) \right] \rightarrow 0$$

$$\frac{\partial F_{A,i}}{\partial \alpha_i} = \frac{F_{A,i}(\alpha_{init} + \Delta \alpha_i) - F_{A,i}(\alpha_{init})}{\Delta \alpha_i}$$

For optimal validation the blade model was scaled by a factor of 1:7.5, leading to a total span of  $b=445.5\text{mm}$  and a chord length of  $c(r/R=0.7)=412.7\text{mm}$  with a maximum thickness of  $t(r/R=0.7)=17.9\text{mm}$ .

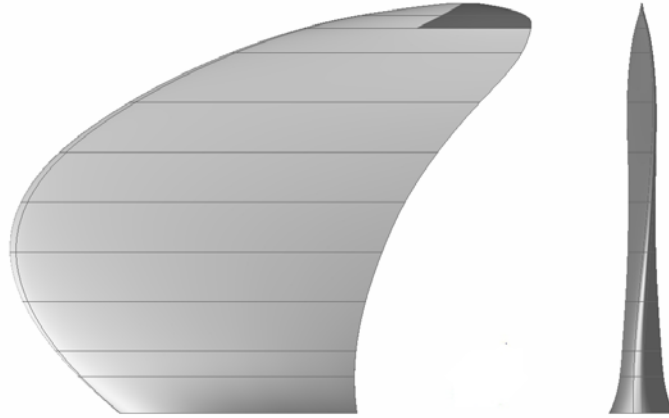


Figure 1: P1380 blade model for translational inflow with tip roughness (dark grey)

The computational domain consists of a block-structured ICEM grid using 19 Mio. hexahedron cells. To ensure grid independent vortex development, the downstream section of the tip was set up with an equally spaced cartesian grid, resolving the vortex cross section by  $56 \times 56$  cells. Calculating the flowfield with the OpenFoam steady state RANS Solver SimpleFoam and a SST turbulence model, the wall function implementation of Tapia [8] was used to model different sizes of sand grain roughness  $h_s^+ = h_s u_\tau / \nu$  in the transitional and the fully rough regime. Within the logarithmic profile

$$u^+ = \frac{1}{\kappa} \ln(y^+) + B - \Delta B$$

the velocity shift for the roughened wall reads

$$\Delta B = \frac{1}{\kappa} \ln \left[ \frac{h_s^+ - 2.25}{87.75} + C_s h_s^+ \right]^{\sin(0.4258(\ln h_s^+ - 0.811))} \quad \text{for } 2.5 \leq h_s^+ \leq 90$$

$$\Delta B = \frac{1}{\kappa} \ln(1 + C_s h_s^+) \quad \text{for } h_s^+ \geq 90$$

The constant  $C_s$ , denoting the roughness type, was found in a series of calculation of the Nikuradse wall friction factor for turbulent pipe flows at  $Re=10^6$ , showing best overall prediction for  $C_s=0.35$  (fig. 2).

According to [5] sand grain roughness elements of  $h_s=(0.5, 0.6, 1.0, 2.0)\text{mm}$  has been considered for suction sided (SS), pressure sided (PS) and suction + pressure sided (SSPS) application areas of  $0.95 \leq r/R \leq 1$  and  $0.5 \leq c_L \leq 1$ . The Reynolds-Number was set to  $Re=10^6$  leading to an inlet velocity  $v_{inlet}=42.3\text{m/s}$ .

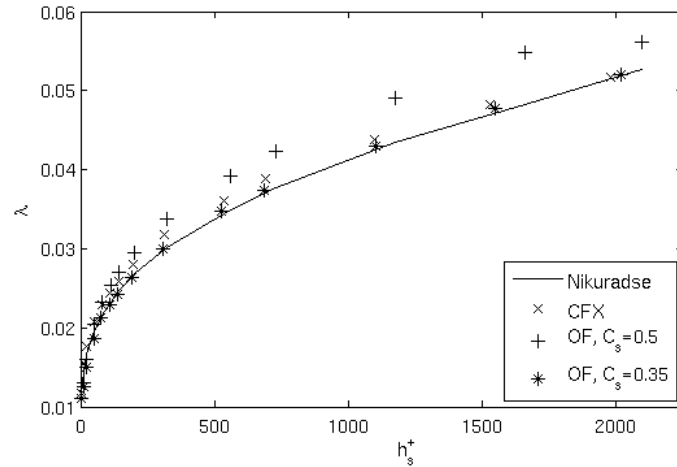


Figure 2: Wall function calculations for wall friction factor in turbulent pipe flows  $Re=10^6$

## Experimental Setup

For validation purpose the pressure and the velocity field within the tip vortex for a smooth and a roughened wing were measured, showing the same dimensions as in the numerical setup. By a single layer of corundum with a mean diameter of  $D_C=0.6\text{mm}$  in an adhesive matrix the roughness structures were applied on either the suction side or the pressure side of the tip region.

The measurement series was carried out at a Goettingen type subsonic wind tunnel, providing a quadratic measurement cross-section of  $2\text{m}^2$ . Integral forces and momentum on the blade model have been recorded by a six-component measurement system. To ensure matching of experimental and simulation data angle of attack and lift of the wing was selected representing the numerical data.

Within a vertical cross section perpendicular to the main inflow direction  $0.5\text{m}$  downstream from the generator line with its center at  $0.427\text{m}$  vertical height 3D Hot-Wire as well as Prandtl Tube measurements were performed. The cross section extended  $165\text{mm} \times 165\text{mm}$  being resolved as in the numerical setup by  $56 \times 56$  measurement points.

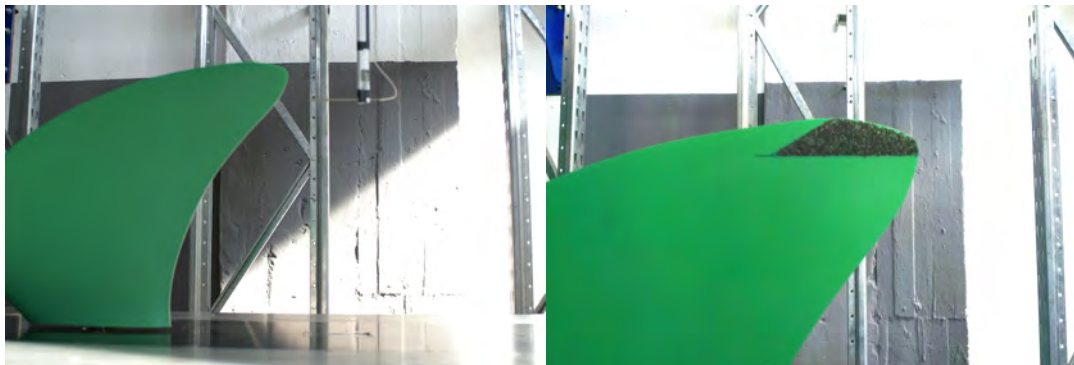


Figure 3: Center of the measurement section for 3D Hot Wire and Prandtl Tube measurements (left); Suction side sand grain roughness on the wing model (right)

## Numerical Results

The simulations showed a distinct relation between type and area of the tip roughness and specific tip vortex parameters. Applying sand grain roughness to the suction side of the tip, the viscous stresses between tip surfaces and adjacent tip vortex were increased, resulting in a damping of the angular momentum and therefore in an increased vortex pressure. The strong pattern of turbulent kinetic energy, forming above the roughened surface, quantifies the losses of rotational energy within the vortex. Depending on the investigated roughness height, the production rate of turbulent kinetic energy exceeds twice as much as for the smooth configuration. Even though the dissipation rate being enhanced as well, leading to an overall reduction of energy contained within the considered system, the turbulent scales dissipate imperfectly. Turbulent fragments tend to roll up into the vortex, shifting the relation between axial and radial cross stresses within the vortex core (fig. 6). For suction sided tip roughness all investigated heights led to an increased vortex core pressure compared to the smooth configuration. Due to additional viscous stresses the overall drag of the blade body rises, while the lift decreases.

Applying sand grain roughness to the pressure side, the tip vortex pressure and angular momentum remains nearly constant compared to the smooth wing, as the viscous effects and vortex are physically separated by the propeller blade. Acting on the boundary layer, the roughened region virtually thickens the blade section in the tip area, increasing the lift slightly. The drag of this configuration is larger than for the smooth wing and for the suction sided roughened wing as well.

Suction and pressure sided tip covered with sand grain roughness show a comparable impact on angular momentum and tip vortex pressure as for the suction sided configuration. Drag and lift nearly superposition from the single sided types, leading to the highest drag of all investigated configurations and lift decreasing slightly compared to the smooth wing.

Calculating the inverse of the glide ratio  $\varepsilon$  one can obtain a decrease in wing efficiency for all setups. These effects become stronger for all configurations as the roughness height increases (fig. 4).

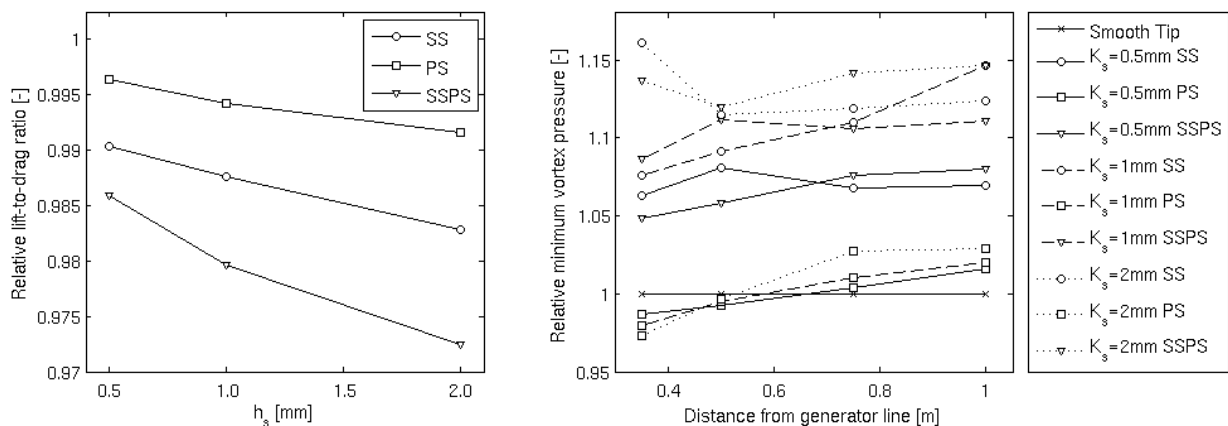


Figure 4: Calculated blade efficiency (left) and tip vortex pressure (right) relative to a smooth wing depending on type and application area of propeller tip roughness

## Experimental Results

For validation purposes the calculations were assisted by a series of wind tunnel measurements, proving the low-pressure region of the tip vortex being effected by the tip roughness depending on the application area. Where for the suction sided tip roughness an increase of about 19% was measured, accompanied by a slightly thickening of the vortex core, the pressure sided tip roughness seems to have no effect on the vortex vacuum. This is surprising somehow, as the measurements showed a significant decrease of the axial velocity suppression within the vortex core for both roughness configurations, with an even stronger effect of the pressure sided tip roughness (suct. side: -11.1%/-8.6%; press. side: -31.1%/-23.3% (Prandtl tube/3D Hotwire)).

Comparing the second order moments for the suction side roughness, a diffusion of the turbulent kinetic energy is observed, thickening the turbulent vortex core (fig. 5). By a closer look at the diagonal Reynolds stresses, an amplification of the axial vortex stresses can be noticed, whereas the radial stresses seem to be diminished. Taking into account that for the given configuration the axial stresses averaging at 1/3 of the radial stresses, the vortex diffusion can be divided into two fractions: First, a thickening of the vortex core by an amplification of the axial stresses, and second, the lowering of the total kinetic energy within the core by

damping the radial stresses (fig. 6). The shifting relation between axial and radial core stresses is also reflected by the experimental data for the cross-correlations, showing an amplification of the correlations between axial and radial fluctuations in opposite to the damping of the correlations between both components of the radial fluctuations.

As the pressure sided roughness showing a similar amplification of the axial stresses, in this case the radial stresses are amplified as well, leading to an overall increase of the turbulent kinetic energy within the vortex core. This is in line with the results observed for the radial cross stresses, being enhanced by the perturbation of the vortex roll up in vicinity of the tip, evidencing a more turbulent vortex structure compared to all other configurations.

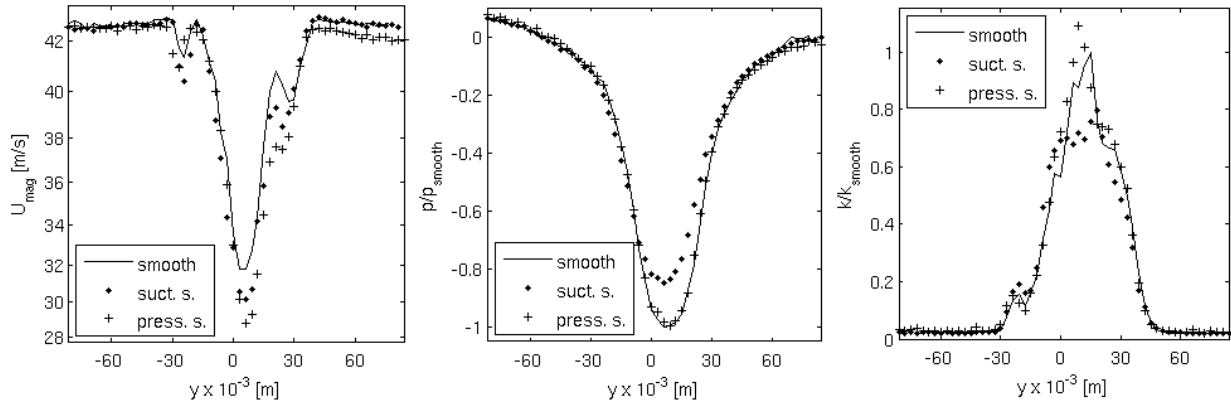


Figure 5: Dynamic pressure (left), static pressure (center) and turbulent kinetic energy (right) for a smooth and a roughened wing ( $h_s=600\mu m$ ) on a horizontal line through the vortex core (distance from generator line  $x=0.35m$ ,  $z=0.427m$ )

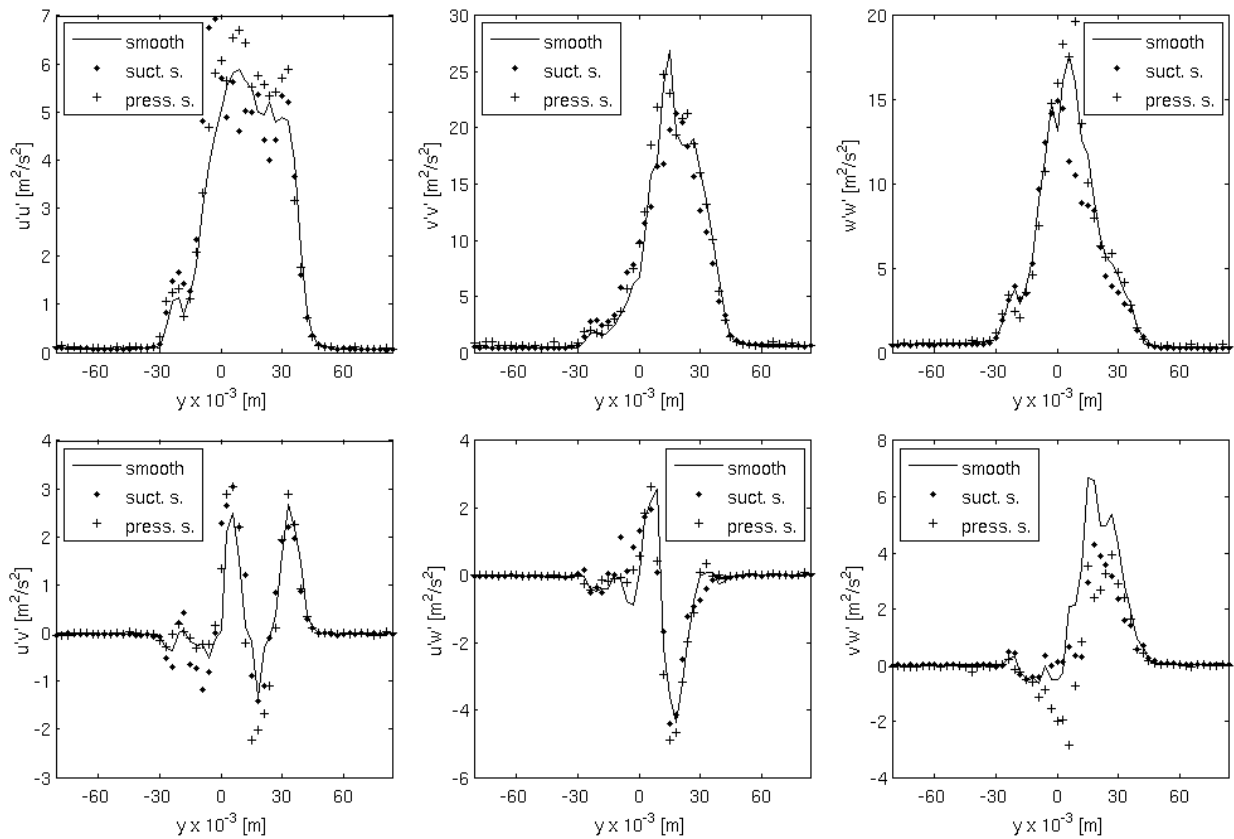


Figure 6: Components of the Reynolds stress tensor for a smooth and a roughened wing ( $h_s=600\mu m$ ) on a horizontal line through the vortex core (distance from generator line  $x=0.35m$ ,  $z=0.427m$ )

## Conclusion

By showing qualitatively good agreement between the different measurement techniques and the simulation results for the resolved vortex structures and the propeller wake, giving a good estimation about peaks and inflection points, a noticeable over estimation of the axial core velocity within the calculations for the smooth as well as the roughened blade can be observed. Examining the resolved pressure field for the smooth configuration a fairly well prediction of the minimum vortex core pressure is presented. Although the pressure increase was suggested by the calculations, an even stronger influence of the roughened tip on the low-pressure region of the tip vortex was measured. It can be seen from the simulation results and the experiments as well, that the stiff correlation between specific propeller thrust and related tip vortex strength can be broken up, using roughened propeller tips.

Considering the suction sided tip roughness to be the most effective solution within this investigation, it can be estimated that by minimized reduction of the open water efficiency due to friction induced losses, cavitation safety in the tip vortex can be improved by nearly 14%.

As this study is concentrated on the physical effects within one-phase flows in the first, all results are going to be validated during the second phase of the project in cavitation tunnel experiments for the rotational propeller model. At the present state of the investigation it can be expected, that the specific application of discrete roughness structures near the propeller tips offers potential to efficient propulsion systems that meets highest industries demands for cavitation-free operation.

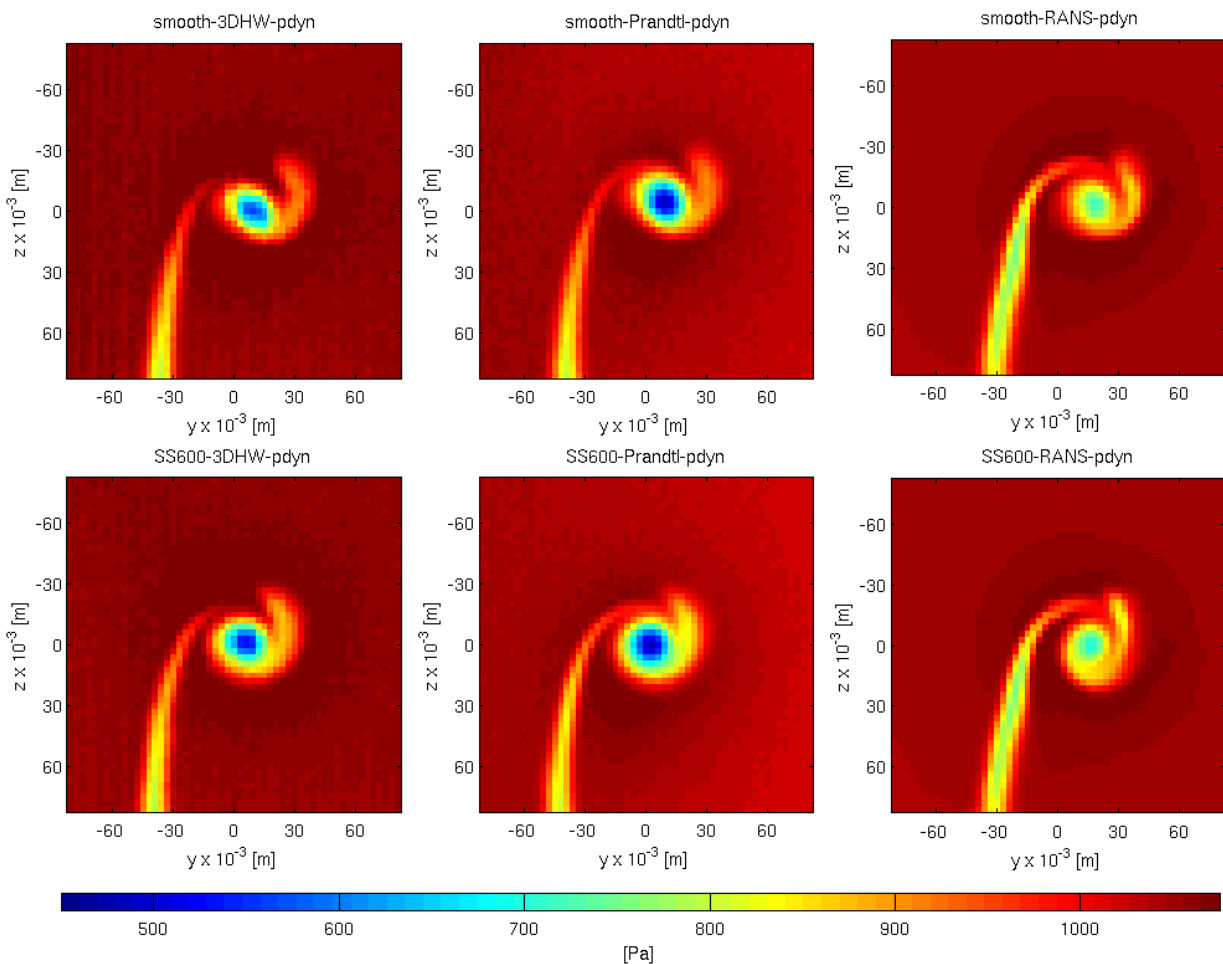


Figure 7: Dynamic pressure from 3D Hot Wire (left), Prandtl Tube (middle) and RANS (right) behind a smooth (top) and a roughened (bottom) propeller tip

## References

- [1] O. Rutgerson C. A. Johnsson. Leading edge roughness - a way to improve propeller tip vortex cavitation. *Propellers and Shafting Symposium*, 1991.
- [2] D. S. Pradeep F. Hussain. Mechanism of core perturbation growth in vortex-turbulence interaction. *12<sup>th</sup> Asian Congress of Fluid Mechanics*, 2008.
- [3] A. Junglewitz J. Friesch. Erocav - improved test methods based on full scale investigations and new theoretical approaches for the prediction of erosion damages. *Summer Meeting STG*, 2003.
- [4] J. Galdo J. Katz. Effect of roughness on rollup of tip vortices on a rectangular hydrofoil. *Journal of Aircraft*, 26, 1989.
- [5] P. Ninnemann O. Philipp. Wirkung von fluegelrauigkeiten auf kavitation und erregung. 2007.
- [6] S. Z. Duan S. I. Green. The ducted tip - a hydrofoil tip geometry with superior cavitation performance. *Journal of Fluids Engineering*, 117, 1995.
- [7] H. S. Koyama T. Watanabe, H. H. Nigim. The effects of propellertip vane on flow-field behavior. *Experiments in Fluids*, 23, 1997.
- [8] X. P. Tapia. Modelling wind flow over complex terrain using openfoam. 2009.
- [9] D. Wittekind. Current status of underwater noise from shipping and the contribution of the propeller. 2011.